https://doi.org/10.5194/essd-2023-195
Preprint. Discussion started: 12 September 2023

Open Access Earth System Science Data Discussions

Annual time-series 1-km maps of crop area and types in the conterminous US (CropAT-US): cropping diversity changes during 1850-2021

Shuchao Ye, Peiyu Cao, Chaoqun Lu

Department of Ecology, Evolution, and Organismal Biology, Iowa State University, Ames, Iowa 5011, USA

Correspondence: Chaoqun Lu (clu@iastate.edu)

Abstract. Agricultural activities have been recognized as an important driver of land use and cover changes (LUCC) and have significantly impacted ecosystem feedback to climate, air, and water quality by altering land surface properties. A reliable historical cropland distribution dataset is crucial for understanding and quantifying the legacy effects of agriculture-related LUCC. While several LUCC datasets have the potential to depict cropland patterns in the conterminous US, there remains a dearth of a high-resolution dataset with crop type details over a long period. To address this gap, we reconstructed historical cropland density and crop type maps from 1850 to 2021 at a resolution of 1 km×1 km by integrating inventory datasets and gridded LUCC products. The results showed that the developed dataset is highly consistent with the county-level inventory data, with an R^2 approaching one and *RMSE* less than 3 Mha (million hectares) at the national level. Temporally, the US total crop acreage has increased by 118 Mha from 1850 to 2021, primarily driven by corn (30 Mha) and soybean (35 Mha). Spatially, the hotspots of cropland shifted from Eastern US to the Midwest and the Great Plains, and the dominant crop types (corn and soybean) moved toward the Northwest of the US. Moreover, we found the US cropping system diversity experienced a significant increase from 1850s to 1960s, followed by a dramatic decrease in the recent six decades under the intensified agriculture. Generally, the developed dataset could facilitate the spatial data development in delineating crop-specific management practices and enable the quantification of cropland change impacts.

https://doi.org/10.5194/essd-2023-195
Preprint. Discussion started: 12 September 2023

Open Access Earth System Science Data Discussions

1 Introduction

Anthropogenic land use and cover change (LUCC) has altered nearly 70% of global ice-free land (Arneth et al., 2019), exerting significant effects on ecosystem services by changing biogeochemical and biophysical processes (Foley et al., 2005; Goldewijk et al., 2017; Johnson, 2013; Betts et al., 2007; Lark, 2023). In particular, agricultural activities have been identified as the dominant driver of LUCC (Cao et al., 2021), with approximately one-third of the land surface altered for agricultural use to meet human demands of food, feed, fiber, and fuel (Zhang et al., 2007). These changes have led to a range of environmental issues, including greenhouse gas emissions (De Noblet-Ducoudré et al., 2012; Yu et al., 2018), agricultural water pollution (Ouyang et al., 2014), and soil degradation (Vanwalleghem et al., 2017). In addition, the intensification of agriculture causes the decline of crop diversity, which can reduce the resilience of crops to various environmental stresses and threaten the crop yield (Burchfield et al., 2019; Gaudin et al., 2015; Renard and Tilman, 2019; Aizen et al., 2019). Therefore, gaining a better understanding of spatiotemporal cropland extent and type changes is critical to quantify the environmental effects of cropland change and promote sustainable agricultural practices (Tilman et al., 2011; Lambin and Meyfroidt, 2011).

As a leading agricultural producer, the conterminous US has experienced a substantial transformation in crop area, distribution, and type over the last two centuries. From 1850s to 1980s, the crop area increased about eightfold from around 20 million hectares to about 160 million hectares, primarily through the conversion of forest, grassland, and other land types (Li et al., 2023; Turner, 1988). Spatially, the development of canals, waterways, and railroads contributed to the cropland expansion to the west (Meinig, 1993). Especially, the Homestead Acts in 1862 played a significant role in stimulating agricultural reclamation. Moreover, in crop commodities, the dominant crop types have shifted. Before the mid-twentieth century, corn and wheat were the dominant crops. However, the cultivated area of soybean has gradually surpassed wheat and became the second widely produced crop type across the US in recent decades (Lubowski et al., 2006). Although these changes have been reported by the government and social scientists (Waisanen and Bliss, 2002), there is still a lack of a long-term cropland dataset to depict the historical crop-specific spatial patterns in the US. Despite that long-term crop-specific management information has been available in the US for quite a long period, large uncertainties remain in developing historical management maps and assessing their environmental and economic consequences spatially, because not knowing “what is planted where” is a big hurdle before the remote sensing data is available.

A wide variety of land use datasets have been used to explore the spatiotemporal patterns of agricultural land in the contiguous US. For instance, History database of global environment (HYDE) (Goldewijk et al., 2017) dataset provides the cropland area in each grid cell from 1000 BC to 2017 AD at a resolution of 5 arc-min. Similarly, Zumkehr and Cambell (2013) developed a cropland distribution dataset at a 5 arc-min resolution from 1850 to 2000. Although these datasets present the long-term land use change history, their coarse resolutions offer limited spatial details. In contrast, the resolution of Cropland Data Layer (CDL), National Land Cover Database (NLCD), and Land Change Monitoring, Assessment, and Projection (LCMAP) is down to 30m. However, their availability and continuity (available in the recent 40 years) are unable to provide historical cropland change patterns. The more recent studies, such as Cao et al. (2021) and Li et al. (2023), developed long-term LUCC datasets at 1 km by 1 km resolution, but the crop type details are missing, making it challenging to recognize the specific crop type change over space and time.

https://doi.org/10.5194/essd-2023-195
Preprint. Discussion started: 12 September 2023

On the other hand, Monfreda et al. (2008) and Tang et al. (2023) generated a global crop type map with more than 170 crop types in the year of 2000 and 2020, and CDL provides the annual crop type distribution in the conterminous US with more than 50 crop types from 2008 to now. Their products also provide information that is only available in the recent two decades, hindering the understanding for historical US crop type development. Overall, the currently available datasets either have short periods, low spatial resolution, or lack specific crop type information, which makes it impossible to assess how crop type changes and crop-specific management before 2000 have affected the climate system and environmental quality at a finer scale. Thus, it is urgent to develop a long-term spatially explicit cropland dataset with crop type details to comprehend the historical US cropland changes.

In this study, we aim to reconstruct the cropland density and crop type maps in the conterminous US from 1850 to 2021 at 1 km by 1 km resolution. The cropland density map presents the distribution and percentage of planted area in each 1 km by 1 km pixel. The crop type map displays the distribution of nine major crop types (corn, soybean, winter wheat, spring wheat, durum wheat, cotton, sorghum, barley, and rice) and one type of "others" (all remaining crop types excluding idle/fallow farm land, and cropland pasture). This study consists of three sections: Section 2 describes the materials and methods used to reconstruct the dataset, Section 3 analyzes the spatiotemporal changes in dominant crop types and crop diversity based on the reconstructed dataset, and Section 4 discusses the differences between our dataset and other datasets, the drivers of cropland change, the implications of US crop diversity change, and the data uncertainty.

2 Materials and method

In this study, we combined three inventory datasets and four gridded datasets to reconstruct the historical cropland density and crop type maps. As illustrated in Figure 1, the entire process involves three stages: reconstructing annual inventory data for each crop type at the county level (Section 2.2), rebuilding cropland density maps (Section 2.3), and generating crop type maps (Section 2.4). In particular, we adopted the following assumptions for reconstructing the cropland maps: (1) the USDA inventory datasets provide the most reliable acreage information for determining cropland area in each county; (2) Cropland data layer (CDL), History database of the global environment 3.2 (HYDE) (Goldewijk et al. 2017), and Land change monitoring, assessment, and projection (LCMAP) provide the potential distribution of cropland, which are used to allocate cropland grids under the control of the rebuilt inventory data (Yu and Lu, 2018); (3) The rotation percentage between corn and soybean linearly increased from 1940 to 2009. The method for acquiring the rotation ratio is introduced in Section 2.4. Furthermore, based on the generated crop type maps, we explored the historical US crop diversity pattern through the diversity index.

https://doi.org/10.5194/essd-2023-195
Preprint. Discussion started: 12 September 2023

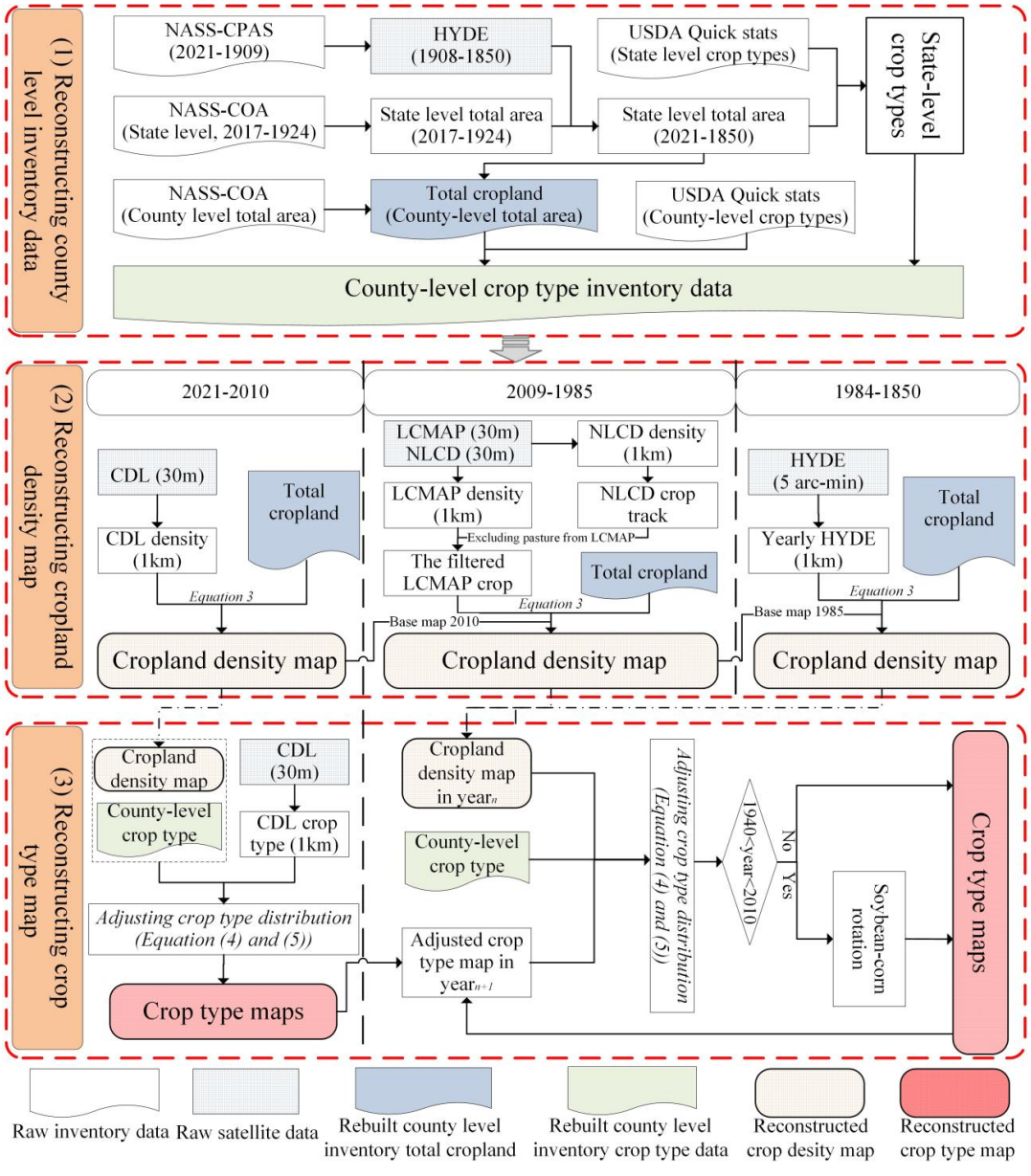

Figure 1. The methodology flow chart. Three boxes with red dashed line correspond to Section 2.2, 2.3, and 2.4, respectively. The county-level total and crop-specific cropland area generated in the box (1) are fed into box (2) and box (3) to reconstruct cropland density and crop type maps, respectively. (NASS-CPAS: Crop Production Annual Summary data from Nation agricultural statistical service of USDA; NASS-COA: Census of Agriculture from Nation agricultural statistical service of USDA; CDL: Cropland data layer; NLCD: National land cover database; LCMAP: Land change monitoring, assessment, and projection; HYDE: History database of the global environment 3.2 (Goldewijk et al. 2017).

https://doi.org/10.5194/essd-2023-195
Preprint. Discussion started: 12 September 2023

2.1 Datasets

Three inventory datasets and four gridded LUCC datasets are used in this study (Table 1). Specifically, NASS-CPAS (Crop Production Annual Summary data from the Nation agricultural statistical service of USDA) and NASS-COA (Census of Agriculture from Nation agricultural statistical service of USDA) provide the total cropland area in each state and each county. USDA-NASS Quickstat is used to track the acreage of specific crop types. These inventory datasets are adopted to reconstruct the historical cropland area. CDL is the most detailed satellite-based cropland dataset, which has been intensively validated by ground truths and other ancillary data with crop classification accuracies up to 90% for major crop commodities (Boryan et al., 2011). Here, we extracted the above-mentioned ten crop types from CDL (Table S1). CDL 2008 and 2009 were excluded due to their low resolution and accuracy compared to other years (Johnson, 2013). NLCD and LCMAP, all derived from Landsat images with a resolution of 30m×30m, were used to provide the cropland spatial information from 1985 to 2009. More specifically, NLCD provides around 5-year cyclical land cover maps from 2001 to 2019, and LCMAP offers annual land use data from 1985 to 2021 (Homer et al., 2020; Xian et al., 2022). Since the cropland in LCMAP includes cropland and pasture, we applied the NLCD-based cropland trajectory to exclude pasture grids in LCAMP (more details presented in Supplementary Methods). HYDE was adopted to offer the potential cropland distribution during 1850-1984. All gridded datasets were resampled to 1km.

Table 1. The gridded and inventory dataset sources.

Data variables (period, resolution)	Properties	Adjustment
CDL (2010-2021, 30m)	The most detailed crop type map. Providing crop type distribution.	Resampled to 1km and reclassified into ten crop types (nine major crop types and one type of "others").
LCMAP (1985-2021, 30m)	Anderson Level I-based legend classification including eight primary land types (Xian et al., 2022). The cropland includes cropland and pasture.	Filtering pasture from cropland based on NLCD crop trajectory.
NLCD (2001-2019, 3-5 years intervals, 30m)	Anderson Level II-based legend including 20 land cover classes (Xian et al., 2022).	Providing cropland distribution.
HYDE 3.2 (1600-2017, 5arc-min)	Including cropland, grazing land, pasture, irrigated rice, etc. Providing cropland distribution.	Linearly interpolation in missing years (1850-1985).
NASS-CPAS (1909-2021)	State-level total planted area.	Gap-filling in missing years (Section 2.2).

https://doi.org/10.5194/essd-2023-195
Preprint. Discussion started: 12 September 2023

NASS-COA (1924-2017, 4-5 years intervals)	State and county-level total cropland area of harvest, failure, and fallow crops.	Gap-filling in missing years (Section 2.2).
USDA-NASS Quickstat (1866-2021)	State and county level planted and harvest area. Including corn, soybean, winter wheat, spring wheat, durum wheat, cotton, sorghum, barley, rice, and all other crop types.	Gap-filling in missing years (Section 2.2).

2.2 Reconstructing historical crop acreage at the county level

By integrating gap-filling multiple inventory and gridded datasets, we reconstructed the total cropland area and the planting area of 9 major crop types in each state from 1850 to 2021. We obtained the area of "others" by calculating the difference between the total cropland area and the summation of plant area of 9 major crops. NASS-CPAS reports the annual plant area of all principal crops for each state from 1909 to 2021, which excludes some minor crop types (such as vegetables and fruits). USDA-COA provides the total area of crop harvest, failure, and fallow for each state from 1925 to 2017 with 4~5-year intervals. We computed the difference between these two datasets for available years and linearly interpolated unavailable years during 1909-2021. The interpolated difference was added to NASS-CPAS to generate the annual state-level total crop plant area from 1909 to 2021. We used the interannual variations of arable land of each state extracted from HYDE to interpolate the total planting area during 1850-1908 (Equation 1).

To identify the planting acreage change for nine major crop types, we obtained the state-level harvest and plant area from USDA-NASS Quickstat. The available harvest and plant areas vary among crop types and states, for which the harvest areas usually have earlier-year reports than those of planting areas (Table S2). The harvest area is highly correlated to plant area in terms of interannual variation. We calculated the ratio of plant area to harvest area for the earliest available year of plant area. We then converted the harvest areas to plant areas by timing the ratio with the harvest areas to extend the plant areas to an earlier period. For the period that the harvest areas are unavailable, we interpolated the plant area from 1850 to 2021 based on the total cropland area generated above (Equation 1 and 2).

We adopted the same approach as for the state-level plant area generated above to obtain the county-level total cropland area and the planting area of 9 major crop types and "others". USDA-COA reports the total county cropland area from 1925 to 2017 with 4~5-year intervals. We gap-filled the total county cropland from 1850 to 2021 by state total cropland area (Equation 1 and 2). Similar to the state-level crop-specific area, we converted the harvest areas to plant areas of 9 major crops in each county from USDA-NASS Quickstat, with varied availability (Table S1). For the period when harvest areas are unavailable, we gap-filled the plant areas during 1850-2021 based on the state-level crop-specific plant area generated above (Equation 1 and 2). The plant area of all other crops ("others") in each county was estimated by calculating the difference between the total cropland area and the total area of 9 major crops.

$$Raw\ data_{i+k} = \frac{Referenced\ trend_{i+k}}{Referenced\ trend_i} \times Raw\ data_i, \quad (1)$$

https://doi.org/10.5194/essd-2023-195
Preprint. Discussion started: 12 September 2023

Open Access Earth System Science Data Discussions

$$Raw\ data_{i+k} = \frac{\text{Referenced trend}_{i+k} \times Raw\ data_i}{Referenced\ trend_i} \times \frac{k-i}{j-i} + \frac{\text{Referenced trend}_{i+k} \times Raw\ data_j}{Referenced\ trend_j} \times \frac{j-k}{j-i}, \quad (2)$$

Where $Raw\ data$ is the raw data that contains missing values, $Referenced\ trend$ is the complete data from which the interannual variations that raw data can refer to, i and j are the beginning and ending year of the gap, $i + k$ is the kth missing year.

2.3 Spatializing county-level cropland density

By incorporating the county-level inventory (Section 2.2) and gridded cropland products, we reconstructed annual cropland density maps with 1 km by 1 km resolution to represent the area and distribution of cultivated land in US from 1850 to 2021. This process was divided into three periods: 2010-2021 (P2010), 1985-2009 (P1985), and 1850-1984 (P1850). CDL, LCMAP, and HYDE were used to provide the potential cropland distribution in P2010, P1985, and P1850, respectively. For the initial density maps in P2010 and P1985, we used a 1 km window to count cropland fraction in each grid resampled from the raw CDL and LMCAP (30m×30m), respectively, while initial annual density maps in P1850 were resampled and linear interpolated from the HYDE maps. The pixel value in the resampled density map, representing the proportion of the cultivated land over the total pixel area, was further corrected based on the reconstructed county-level inventory data (Equation (3)).

Specifically, when the total cropland area in a county from the initial density map is larger than that of the inventory area, the extra area from all grid cells in the initial map would be deducted to keep consistent with the magnitude of the inventory data; On the contrary, if the cropland area was less than the inventory data, the inadequate area would be added to all pixels (Yu and Lu 2018). If the fraction in a grid is reduced below zero, the cropland fraction in that grid is assigned to zero and the remaining difference area between the map and the inventory data is subtracted from other grids. Conversely, if the fraction in a grid increases above one (100%), then the value in that grid is assigned to one, and the remaining area will be added to other grids.

$$AdjPixel_k = Pixel_k + \frac{(inv - \sum_1^n Pixel_k)}{n}, \quad (3)$$

Where n is the total number of valid cropland pixels in a county; k is the pixel ID in that county, which is from 1 to n; inv is the inventory crop area in that county; $Pixel_k$ is the initial cropland density in pixel k; $AdjPixel_k$ is the adjusted cropland density in pixel k.

To eliminate the gap between CDL and LCMAP, we used the adjusted CDL 2010 density map as a baseline map to retrieve the cropland density maps during 1985-2009 by adopting the year-to-year gridded changes from the resampled LCMAP maps. Taking developing the density map in the year 2009 as an example, we first calculated the annual difference in each grid from 2009 to 2010 based on the LCMAP density maps. Then, we applied that difference to the adjusted CDL 2010 map to generate the density map 2009 with keeping the cropland area consistent with the inventory area. Following the same rule, the adjusted LCMAP 1985 was used to retrieve the density maps in P1850.

https://doi.org/10.5194/essd-2023-195
Preprint. Discussion started: 12 September 2023

Open Access Earth System Science Data Discussions

2.4 Spatializing county-level crop type map

Based on the reconstructed county-level crop type inventory data (Section 2.2), corrected cropland density maps (Section 2.3), and CDL, spatializing annual crop type maps was divided into two periods: 2010-2021 (P1) and 1850-2009 (P2). For P1, the raw 30m resolution CDL crop type maps were resampled to 1 km to provide the potential crop type distribution. In this process, we assigned the resampled grid to a type with the biggest percentage in a 1 km window. By integrating resampled crop type maps and reconstructed cropland density maps, we counted the total area for each type at the county level and identified specific crop types with a greater area than the inventory data. We further converted the surplus area from these types to other types (Equation 4 and 5). In particular, considering the natural planting scenario, the surplus area was randomly selected for converting to other types to avoid a grid planted by a fixed type. For P2, we assumed that the crop type pattern in two consecutive years wouldn't change significantly, and used the rebuilt crop type map in $year_{i+1}$ to provide the potential crop type distribution in $year_i$. Then, we followed the same rule in P1 to reconstruct the crop type map in $year_i$.

$$AdjType_j = inv_j - \sum_1^n (AdjPixel_{j_k}), \tag{4}$$

Where j is the crop type ID ranging from 1 to 10, which is identified from the initial crop type map; n is the number of total valid pixels in crop type j; k is the pixel ID of crop type j ranging from 1 to n identified from the initial crop type map; inv_j is the inventory area of type j; $AdjPixel_{jk}$ is the adjusted cropland percentage in pixel k; $AdjType_j$ is the crop area converted to other types; For $year_i$ between 2010 and 2021, the initial crop type map is resampled from CDL; For $year_i$ from 1850 to 2009, crop type map is the adjusted crop type map in $year_{i+1}$.

$$\begin{cases} Converting\ the\ area\ of\ AdjType_j\ from\ type\ j\ to\ other\ types, if\ AdjType_j < 0; \\ Converting\ the\ area\ of\ AdjType_j\ from\ other\ types\ to\ type\ j, if\ AdjType_j > 0; \end{cases} \tag{5}$$

Considering the dominant crop rotation type in US, soybean and corn rotation, we simulated corn-soybean rotation from 1940 to 2009 by randomly converting a certain area between corn and soybean according to the rotation rate. Based on CDL crop maps, we calculated the rotation rate as the ratio of the area where corn-soybean conversion occurred to the total corn-soybean area between the two consecutive years during 2010-2021 (Yu et al., 2018). To get a more reliable rotation rate, we did a rotation operation on the county where the corn-soybean rotation occurred no less than seven years from 2010 to 2021 and assigned the average value as the rotation rate of the 2010s. Because soybean was rarely planted in the Corn Belt before 1940, we assumed that the rotation rate linearly increased from 0 in 1940 to that average value in 2010 (Yu et al., 2018).

2.5 Crop diversity analysis

Crop diversity has been identified as a potential factor affecting crop yield (Renard and Tilman, 2019; Driscoll et al., 2022). Here, we adopted a true diversity proposed by Jost (2006) to analyze the US crop diversity pattern. The true diversity (D) quantifies the effective number of crop species (Equation 6), where a given D value is equivalent to D species occupying an equal area in a certain space. D is calculated as the exponent of Shannon diversity index (H).

$$D = \exp\left(-\sum_{j=1}^{n}(P_j * lnP_j)\right) = \exp(H), \tag{6}$$

https://doi.org/10.5194/essd-2023-195
Preprint. Discussion started: 12 September 2023

Where, P_j is the proportion of the cropland area occupied by crop type j over the total cropland area, and n is the number of crop species. In this study, the diversity calculated involves ten crop types, including nine major crop types and a category of "others".

3 Result

3.1 Validation of the data products

To validate the developed maps, we compared the annual crop type-specific acreage extracted from our maps with the raw inventory data at county level in 1920, 1960, 2000, and 2020 (Figure 2). The county-level acreages derived from our products and inventory data are close to the 1:1 line, with R^2 exceeding 0.95 and *RMSE* < 1 Kha for all the major crop types except for winter wheat (R^2 = 0.98, *RMSE* = 2.79 Kha) and cotton (R^2 = 0.95, *RMSE* = 3.97 Kha). Although winter wheat and cotton present a relatively greater *RMSE*, the counties with crop area bias greater than 10% only account for 9.7% and 6.1% of total winter wheat- and cotton-planting counties in the selected four years, respectively. We further examined the consistency in national crop-specific acreage between our maps and the rebuilt inventory data during 1850-2021 (Figure S1). The results show that the map products match well with the inventory data (R^2 close to 1 and *RMSE* < 0.3 Mha for all crop types), indicating that the developed maps are highly consistent with the inventory data. The validations indicate that the cropland area from the developed dataset is highly reliable both at the national and county level.

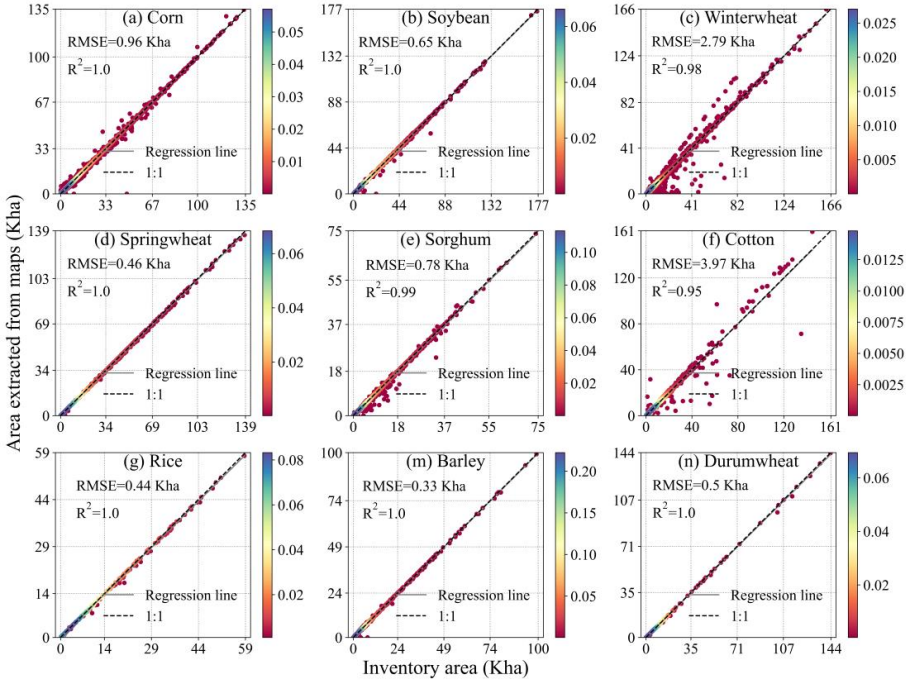

Figure 2. Comparison of crop-specific cropland area between reconstructed maps and raw inventory data at county level in 1920, 1960, 2000, and 2020 (Kha is thousand hectares). The color bar in each subfigure indicates the probability density of paired point calculated by the gaussian kernel.

https://doi.org/10.5194/essd-2023-195
Preprint. Discussion started: 12 September 2023

3.2 Temporal changes in crop-specific areas

We examined the historical cropland area changes among crop types in the US from 1850 to 2021 (Figure 3). In general, the US cropland expanded rapidly from 21.73 Mha in 1850 to 149.38 Mha in 1919, followed by a wide fluctuation ranging from 134.78 Mha to 161.80 Mha until 1990, and then kept relatively stable around 140.00 Mha until 2021. Corn was the dominant crop in the US, accounting for more than 20% of national total cropland area throughout the study period. Temporally, it rose sharply from 7.47 Mha in 1850 to 50.51 Mha in 1917, followed by a continuous drop to 26.34 Mha until 1962, and slowly increased to 37.75 Mha during 1962-2021. Soybean soared significantly from 4.38 Mha in the 1940s to 35.25 Mha in 2021, becoming the second most extensive crop type in the US. Winter wheat constantly increased from 3.25 Mha in 1850 to 26.48 Mha in 1981 and then dropped to 12.88 Mha in 2021, while spring wheat fluctuated dramatically after it plateaued at 8.29 Mha in 1933. Barley and sorghum climbed to peaks of around 8 Mha in 1940s and 11 Mha in 1950s, and then dropped to about 1 Mha and 3 Mha by 2021, respectively. Besides, cotton and durum wheat both reached their peaks before the 1930s and then fell to a relatively stable level. Throughout the study period, the total US cropland increased by 118 Mha, predominantly driven by corn (30 Mha), soybean (35 Mha), and others (31 Mha). The remaining row crops shared about 18% of this increase, including winter wheat (9.6 Mha), spring wheat (4.5 Mha), sorghum (2.7 Mha), cotton (2.8 Mha), and rice (1 Mha).

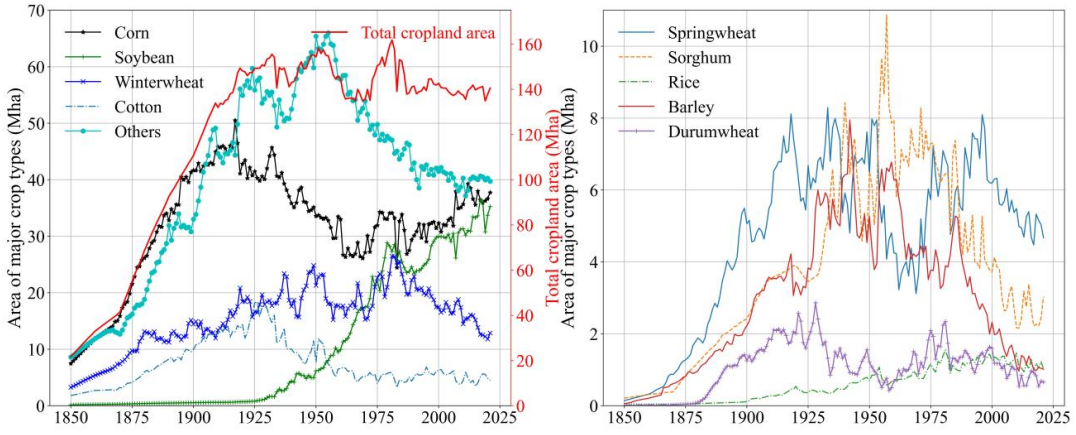

Figure 3. Annual area of major crop types and total US cropland area from 1850 to 2021.

3.3 Dynamics of cropland distribution

The spatial patterns of cropland density and crop type are presented in Figure 4. The results show that the cropland was mainly distributed in the eastern region of the US in 1850 with a low distribution percentage (< 40%) (Figure 4(a)). Then, the cropland density enhanced substantially (40%-80%) in 1900 (Figure 4(b)). Meanwhile, a large area of the Great Plains (the spatial pattern of US subregions showed in Figure 5(2-a)) was cultivated to plant corn and spring wheat in the Northern Great Plains and winter wheat in the Southern Great Plains during 1850-1900 (Figure 4(f)). From 1900 to 1950, the cropland fraction was continuously elevated (>60%) (Figure 4(c)), especially in the Midwest and the Great Plains. During 1950-2021, spring wheat expanded westward to Montana (Figure 4(h)), enhancing the cropland fraction in the Northern Great Plains. Moreover, the category of "others" substantially

https://doi.org/10.5194/essd-2023-195
Preprint. Discussion started: 12 September 2023

substituted corn, winter wheat, and cotton in the Southeast of US, and lowered the cropland density in this region (Figure 4(d)). It was noted that the soybean increased tremendously since 1950 in the Midwest, the Dakotas, and the rice belt, replacing parts of spring wheat, winter wheat, barley, and rice in these regions. Overall, the hotspots of US cropland have shifted from the Eastern US to the Midwest and the Great Plains with the increasing cropland percentage over the past 170 years.

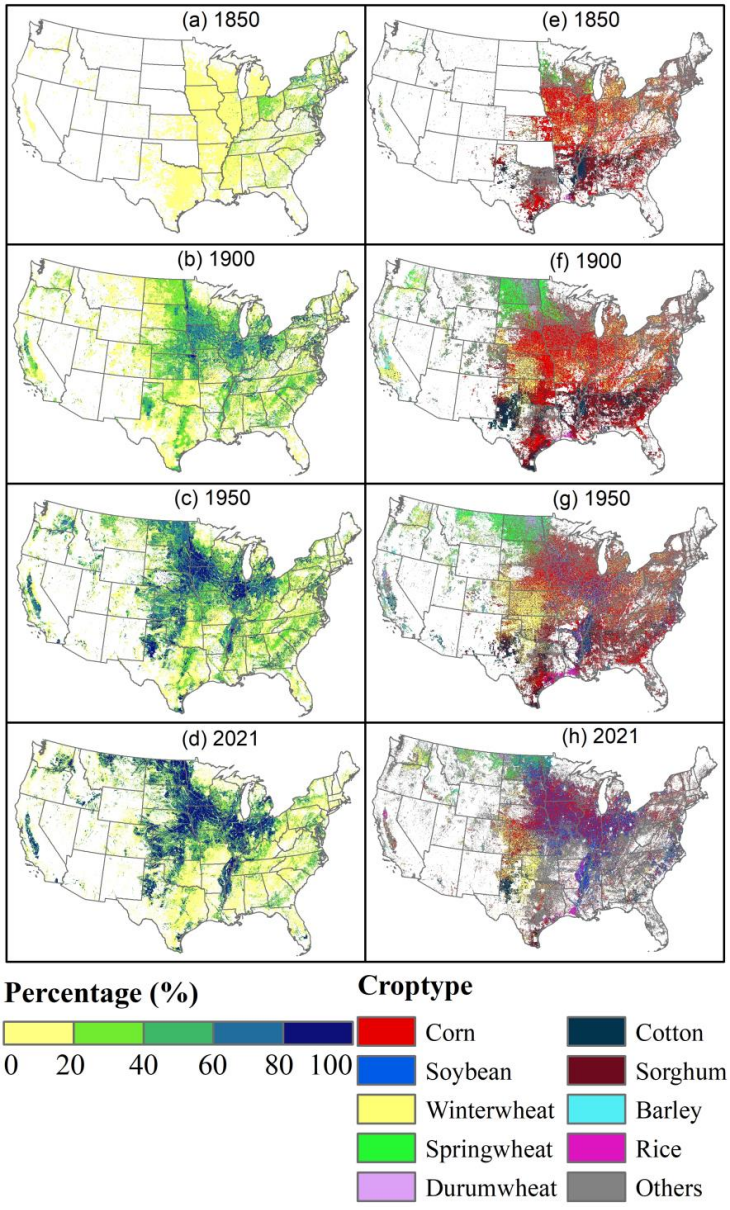

Figure 4. The spatial patterns of cropland percentage (a-d) and crop type (e-h) at 1 km by 1km resolution in 1850, 1900, 1950, and 2021. The color bar of "Percentage" indicates the percentage of cultivated area to the grid area. "Others" represents the remaining crop types.

https://doi.org/10.5194/essd-2023-195
Preprint. Discussion started: 12 September 2023

Furthermore, the spatiotemporal patterns of each major crop type were examined in this study to present a systematic understanding of the US cropland extent and type changes (Figure 5, Figure S2 and S3). Specifically, corn was mainly planted in the east in 1850, with a low cropland fraction (<40%) (Figure 5(1-a)). Then, it gradually expanded to the Great Plains, and the total area increased by 40.34 Mha from 1850 to 1917. Meanwhile, the hotspots of corn planting areas shifted to the Midwest, the southeast of the Northern Great Plains, and the northeast of the Southern Great Plains (Figure 5(1-b)). From 1917 to 1962, the spatial extent of corn had shrunk in South Dakota, Nebraska, Kansas, and the Southeast, with a total area decrease of 24.17 Mha (Figure 5(1-c)). Although the Southeast experienced a large decline in corn acreage during 1962-2021, the planting density of corn significantly increased in the Midwest and the southeast of the Northern Great Plains, resulting in the corn area peaking at 37.75 Mha in 2021 (Figure 5(1-d)).

Temporally, soybean was rarely cultivated in the US from 1850 to 1900 with a total area less than 1 Mha (Figure 5 (2-a and 2-b)). During 1900-1940, the planting area of soybean had a small expansion in the Midwest, with a total area rising to 4.38 Mha (Figure 5(2-c)). But then, it had a dramatic expansion from 1940 to 2021 to the Midwest, Southeast, and the east of Northern Great Plains, with the total soybean area increasing to 35.25 Mha (Figure 5(2-b)).

Winter wheat was mainly located in the Midwest in 1850 with a total area of 3.25 Mha (Figure 5(3-a)). In the following five decades, it spread to the Great Plains, California, Washington, and Oregon, with the total area increasing to 14.45 Mha in 1900 (Figure 5(3-b)). From 1900 to 1981, although its spatial extent had shrunk in Midwest, it expanded significantly in the Southern Great Plains, the Southeast, and Montana (Figure 5(3-c)). Meanwhile, the cropland density also enhanced in this period. These changes led to the planting area of winter wheat reaching the peak of 26.48 Mha in 1981. However, during 1981-2021, a large area of winter wheat was replaced by other crop types or other land use types in the Midwest, Southeast, Montana, Washington, and California (Figure 5(3-d)), which reduced the total area of winter wheat to 12.88 Mha in 2021.

Cotton was mainly distributed in the Southeast in 1850 with a low density (Figure S2(1-a)). It sharply expanded to the Southern Great Plains and California with the increased density during 1850-1925 (Figure S2(1-b)), and the total area of cotton increased by 10.80 Mha in this period. But the period of 1925-2021 was characterized by a huge contraction of cotton area in the Southeast and Southern Great Plains, with a total area declining to 4.50 Mha (Figure S2 (1-c and 1-d)).

For spring wheat, it significantly spread from Montana and Wisconsin to the Midwest and Northwest during 1850-1933, with the total area increasing to 8.29 Mha (Figure S2 (2-a) and (2-b)). But the distribution of spring wheat had largely shrunk in the Midwest and Northwest from 1933 to 1969 (Figure S2 (2-b) and (2-c)), resulting in the area decreasing to 3.12 Mha. In recent decades, it mainly centered in the northern part of the Northern Great Plains with the enhanced density in each grid, and its total area increased to 4.67 Mha in 2021 (Figure S2 (2-d)).

Sorghum consistently expanded in the Southern Great Plains from 1850 to 1957, and its total area increased by 10.66 Mha (Figure S3 (1-a to 1-c)), followed by an area decline thereafter, which left the total area at 3.03 Mha in 2021 (Figure S3 (1-d)). Similarly, barley experienced a continuous expansion in the Midwest, Great Plains, Northeast, California, and Colorado, with the total area rising from 0.06 Mha in 1850 to 7.94 Mha in 1942 (Figure S3 (2-b to 2-

https://doi.org/10.5194/essd-2023-195
Preprint. Discussion started: 12 September 2023

c)). However, between 1942 and 2021, the distribution of barley had a dramatic contraction across the entire US and shrank to 1.02 Mha in 2021, with a small extent in the Northern Great Plains (Figure S3 (2-d)).

Compared with other major crop types, both the distribution of durum wheat and rice only occupied a small area of the US over the entire study period (<3 Mha). Specifically, durum wheat experienced a great expansion in the North Dakota and South Dakota from 1850 to 1928 (Figure S2 (3-a and 3-b)), and its area reached a peak of 2.87 Mha in 1928. However, it contracted to the eastern part of North Dakota during 1928-1958 with a total area declining to 0.42 Mha (Figure S2 (3-c)), then its planting area shifted to the junction of North Dakota and Montana from 1958 to 2021 (Figure S2 (3-d)). Rice consistently expanded in Arkansas, Louisiana, Mississippi, and Texas from 1850 to 1981 with a total area increase of 1.53 Mha (Figure S3 (3-a to 3-c)), gradually forming the current rice belt pattern, followed by a small shrinkage (0.52 Mha) in these regions between 1981 and 2021 (Figure S3 (3-d)). The category of "others" includes many other minor crop types (peanuts, oats, alfalfa, etc.), which accounts for 27%~43% of the total US cropland area and is distributed across the entire US (Figure S4).

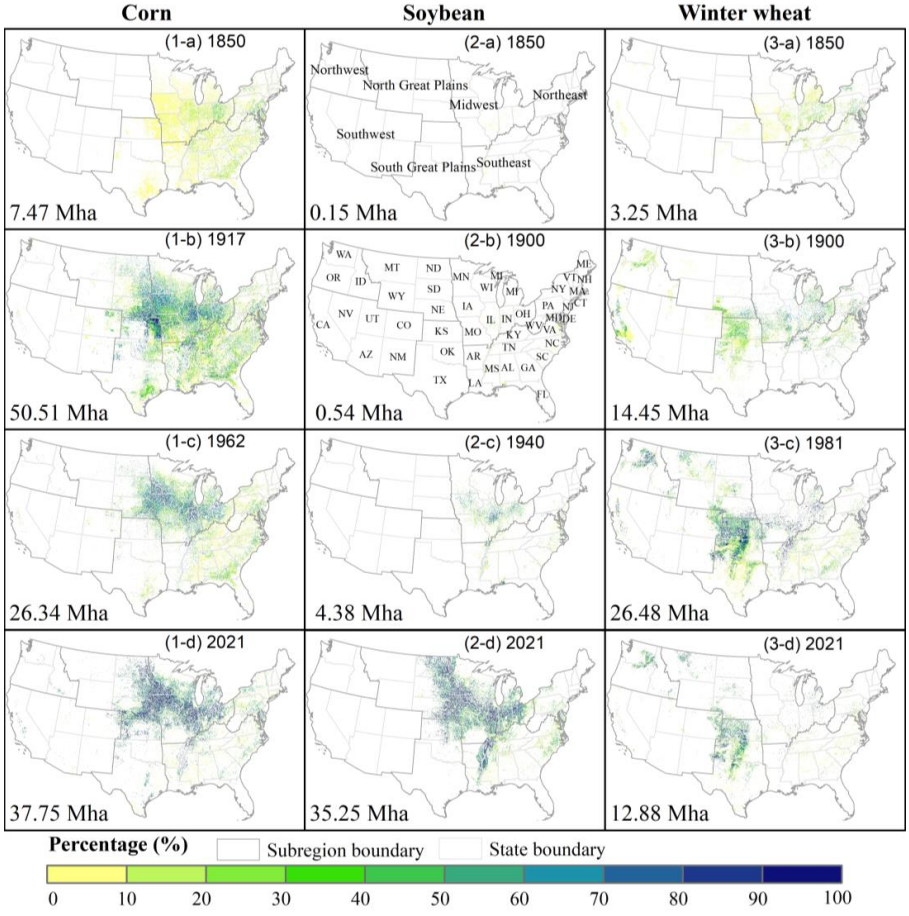

Figure 5. The spatial density pattern of corn, soybean, and winter wheat at 1km by 1km resolution in the area turning years. The first, second, and third columns are the density pattern of corn, soybean, and winter wheat, respectively.

https://doi.org/10.5194/essd-2023-195
Preprint. Discussion started: 12 September 2023

The total planting area for each crop type is presented in the bottom left of each subfigure. The color bar at the bottom indicates the percentage of cultivated area to the total grid area.

3.4 Changes in cropping diversity over time

Here, the value of true diversity (*D*) is interpreted as the number of crop species with an equal area in a certain space (L Jost, 2006; Hijmans et al., 2016), so a higher D value reflects more crop types, or more even distribution, or both. As shown in Figure 6, the US cropping system diversity had undergone dramatic change over time, with a sharp increase from 1850 to 1963 and a significant decline in the recent 60 years. Among different regions, the Southwest, Northern Great Plains, Southern Great Plains, and Southeast had a higher cropping system diversity than the remaining regions. Specifically, the diversity in Southwest, Southern Great Plains, and Northern Great Plains presented a similar change during 1850s-1940s, with a drop from 1850s to 1880s followed by an obvious increase to 1940s (Figure 6 (b)). Starting from 1940s, the diversity in Northern Great Plains peaked around 1990s and then constantly decreased to 2021, while Southern Great Plain's diversity presented an opposite trend in this period. Meanwhile, Southwest witnessed a continuous decline in crop diversity from 1940s to now. The Southeast kept its diversity stable during 1850s-1930s and then experienced a significant increase from 1940s to 2000s. However, in the recent 20 years, the diversity in Southeast dropped sharply. The diversity in Northeast showed an increase trend across the entire study period. Northwest's crop diversity fluctuated between 2.5 and 3 from 1850s to 1970s and then had a continuous increase to now. Midwest's crop diversity kept relatively stable during 1850s-1920s. After increasing to its peak between 1920s and 1930s, it kept stable from 1930s to 1980s, followed by a dramatic decrease to 2021.

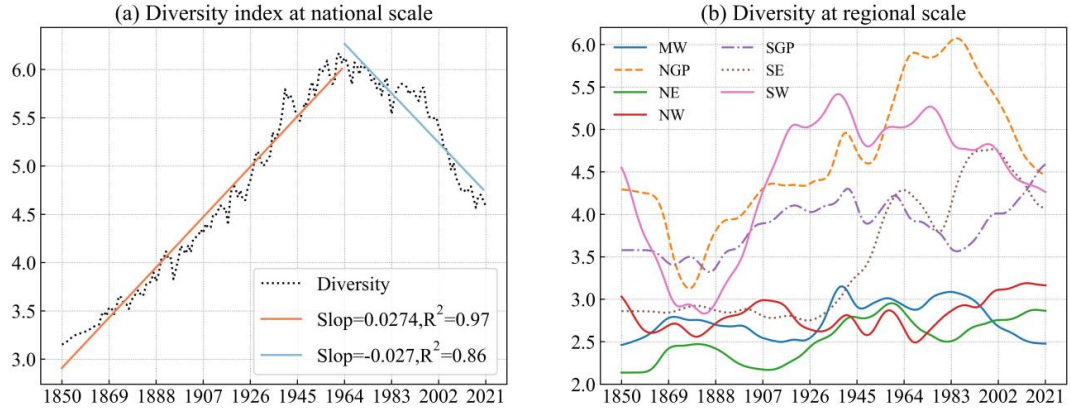

Figure 6. The temporal trend of diversity value in US (a) and seven regions (b). NW, SW, NGP, SGP, MW, SE, and NE are the abbreviation of Northwest, Southwest, Northern Great Plains, Southern Great Plains, Midwest, Southeast, and Northeast, respectively. The spatial map of seven regions is presented in Figure 5 (2-b). To get a better visual pattern, the trends of seven regions in (b) were smoothed by the gaussian function. The diversity value is calculated based on the reconstructed inventory data.

https://doi.org/10.5194/essd-2023-195
Preprint. Discussion started: 12 September 2023

4 Discussion

4.1 Comparison with other datasets

We compared the data products from this study and previous works in terms of the historical total cropland area in the US (Figure 7) and their spatial patterns (Figure 8). By combining NASS-CPAS and NASS-COA to reconstruct state- and county-level inventory data, the US total cropland area derived from our density maps matches well with that from NASS-CPAS from 1850 to 1940 and aligns consistently with the magnitude of NASS-COA and the interannual variations of NASS-CPAS between 1940 to 2021 (Figure 7). We extracted the US total cropland area from two widely used geospatial satellite products (USDA-CDL and USGS-NLCD) in recent two decades. These two datasets demonstrate a smaller area than that of NASS-CPAS before 2017, whereas the magnitude and interannual variation of their estimations were more consistent with this study in the recent five years. Meanwhile, Yu and Lu (2018) and Li et at. (2023) all used NASS-CPAS to develop CONUS and YLMAP, respectively, resulting in a lower US total cropland area after 1940 than this study. This is because the NASS-CPAS only includes the cropland area of principal crops in each state, which is lower than the total cropland area reported by NASS-COA, especially after 1940. Among the existing databases, LCMAP, HYDE, GBC, and ZCMAP represented an upper bound of the US total cropland area. Especially for GBC, it reported the national total crop acreage about 50% higher than the upper range of all other data products (~300 Mha vs ~200 Mha around the 1980s in Figure 7).

The divergence among these data products is mostly caused by different cropland definitions and cropland map generation processes. Specifically, the category of cropland in LCMAP and ZCMAP contains crop and pasture (Zumkehr and Campbell, 2013; Xian et al., 2022), while the cropland in HYDE and GBC includes arable land (Goldewijk et al., 2017; Cao et al., 2021), leading to their higher cropland area than our result (Figure 7). Spatially, we found that the fraction in each grid from HYDE is higher in many low-density regions than our products, such as Northwest, Southeast, and Southwest (Figure 8 and the first row in Figure 9). This might be related to the weighting maps used to allocate cropland for each grid in HYDE, which heavily rely on social and natural indicators (Yu and Lu, 2018; Klein Goldewijk et al., 2011). Similarly, the grid density of ZCMAP was also higher than this study in low-density regions (the first row in Figure 9) because ZCMAP adopted an assumption that the historical spatial crop pattern kept roughly similar to the basemap 2000, in which the fraction in each grid is higher in these regions (Ramankutty et al., 2008; Zumkehr and Campbell, 2013). Moreover, CONUS showed a more extensive cropland distribution than our maps (especially in the Great Plains and Southeast, Figure 8 and the third row in Figure 9). This is likely because they produced more potential cropland grids than the county records through an artificial neural networks-based land cover probability occurrence model (Li et al., 2023). GBC feeds population density and eight biophysical variables (including elevation, temperature, soil water, etc.) into a random forest model to generate the cropland distribution (Cao et al., 2021). As a result, the spatial pattern between GBC and our maps shows a high agreement at the national scale (Figure 8). However, the cropland percentage in each grid cell of GBC is significantly higher than other maps (Figure 8 and the second row in Figure 9), which might be related to the base map used in their study and the lack of inventory records for limiting the total cropland area in US (Cao et al., 2021).

In terms of spatial details among these datasets, our products, YLMAP, CONUS, and GBC (1km×1km) can provide more detailed spatial information than HYDE and ZCMPA (5 arc-min) (Figure 9). Furthermore, compared

https://doi.org/10.5194/essd-2023-195
Preprint. Discussion started: 12 September 2023

with YLMAP, CONUS, and HYDE incorporating state-level census, our products are likely to demonstrate more reliable cropland density heterogeneity within state (the third row in Figure 9) since we adopted county-level census to control the total cropland area in each county. Thus, the rebuilt map is capable of capturing spatial shifts between counties within a same state, such as cropland abandonment in some counties but expansion in others (Li et al., 2023). This indicates that the county inventory-derived datasets are more appropriate for subregion applications (Yang et al., 2020).

Overall, our product keeps highly consistent with the county-level inventory data and presents similar cropland distribution to YLMAP and GBC that involves both biophysical and socioeconomic drivers to generate crop pixels. In addition, unlike cropland involving arable land in HYDE or harvest land in CONUS mentioned above, the definition of cropland in our product refers to the planting cropland and excludes idle/fallow farm land and cropland pasture, providing real surface information disturbed by agriculture. This can improve the accuracy of estimating cropland change's effect on the environment. Therefore, the developed maps can provide a more comprehensive cropland tracking for ecological and environmental applications both on the cropland distribution and cropland area at national and regional scales.

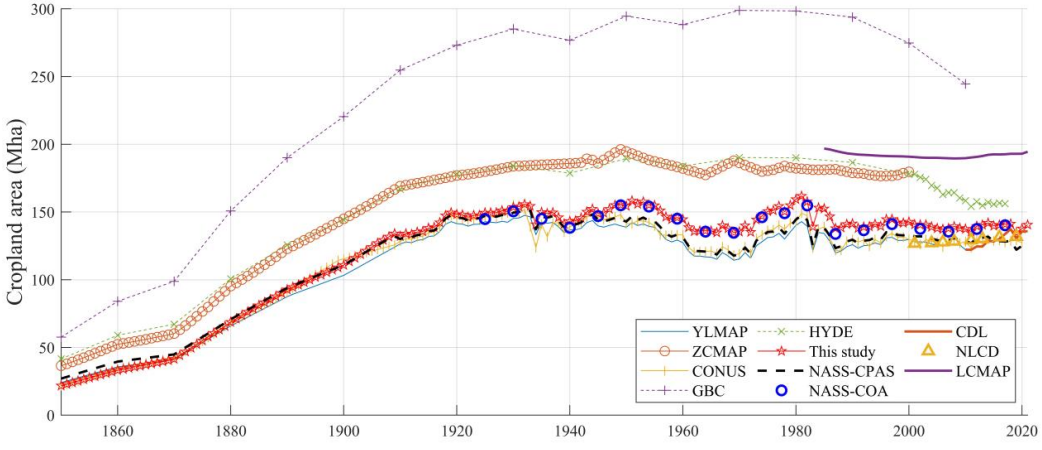

Figure 7. Comparison of the US total cropland area from different sources. CDL: Cropland data layer; NLCD: National land cover database; LCMAP: Land change monitoring, assessment, and projection; YLMAP: the US cropland map from Yu and Lu (2018); ZCMAP: the US cropland map from Zumkehr and Campbell (2013); CONUS: the cropland map from Li et al.(2023); GBC: the US cropland extracted from the global cropland dataset developed by Cao et al. (2021); HYDE: History database of the global environment 3.2 (Goldewijk et al., 2017); NASS-CPAS: the Crop Production Annual Summary data from Nation agricultural statistical service of USDA; NASS-COA: the Census of Agriculture from Nation agricultural statistical service of USDA.

https://doi.org/10.5194/essd-2023-195
Preprint. Discussion started: 12 September 2023

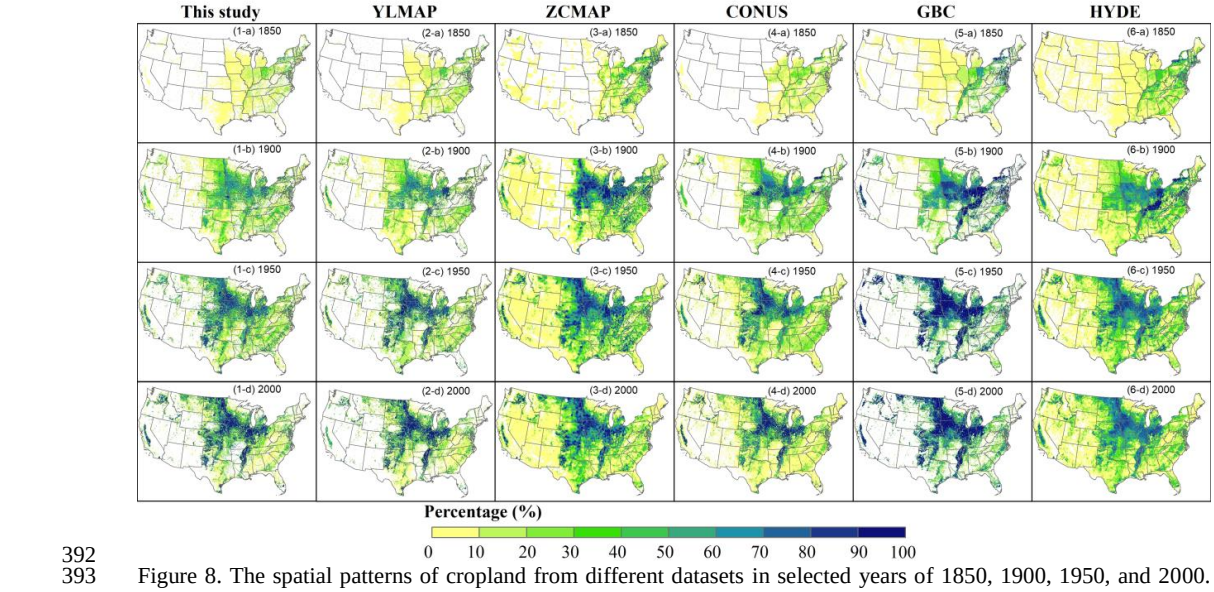

Figure 8. The spatial patterns of cropland from different datasets in selected years of 1850, 1900, 1950, and 2000. YLMAP (1km): the US cropland map from Yu and Lu (2018); ZCMAP (5 arc-min): the US cropland map from Zumkehr and Campbell (2013); CONUS (1km): the cropland map from Li et al. (2023); GBC (1km): the US cropland extracted from the global cropland dataset developed by Cao et al. (2021); HYDE (5 arc-min): History database of the global environment 3.2 (Goldewijk et al. 2017).

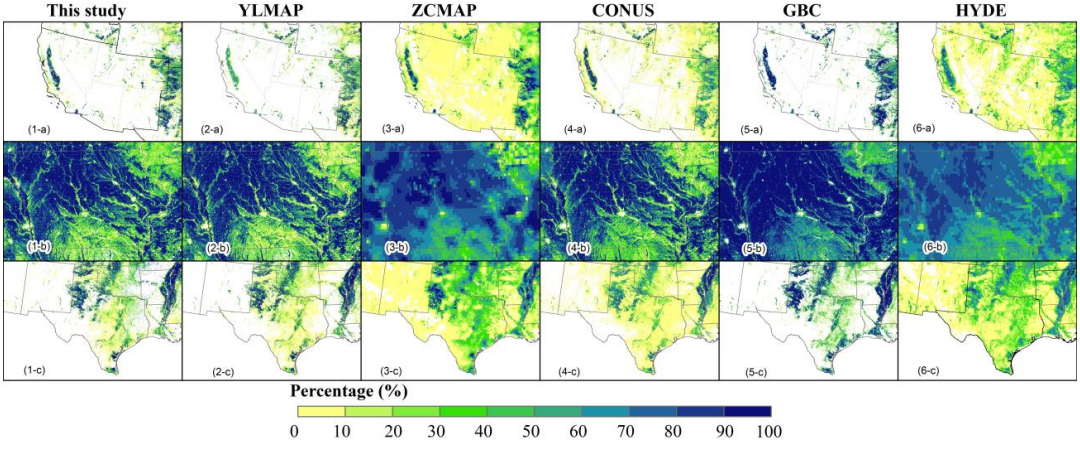

Figure 9. The detailed spatial pattern from different datasets in the year 2000. YLMAP (1km): the US cropland map from Yu and Lu (2018); ZCMAP (5 arc-min): the US cropland map from Zumkehr and Campbell (2013); CONUS (1km): the cropland map from Li et al. (2023); GBC (1km): the US cropland extracted from the global cropland dataset developed by Cao et al. (2021); HYDE (5 arc-min): History database of the global environment 3.2 (Goldewijk et al. 2017). The spatial extent in each row from (a) to (c) is Southwest, Iowa, and Texas, respectively.

4.2 The drivers for US cropland change

Between 1850 and 1900, there was a notable cropland expansion toward the west (Figure 4). This was mainly driven by the Homestead Act of 1862, which provided 160 acres of land to the public for farming purposes (Anderson,

https://doi.org/10.5194/essd-2023-195
Preprint. Discussion started: 12 September 2023

2011). Additionally, the end of the Civil War, the disbanding of armies, and the building of canals and railroads toward the west, further contributed to the agricultural market and export, accelerating agricultural reclamation (Ramankutty and Foley, 1999). At the same time, corn, cotton, and wheat were the dominant crop types and expanded rapidly to the west (Figure 5 and Figure S2). From 1900 to 1950, advanced irrigation systems, industrial technology, and mechanization further promoted agricultural development. For instance, the areas of winter wheat, sorghum, and barley increased substantially in this period (Figure 5 and Figure S2-S3). Subsequently, the fluctuation of the market, policy structure, and weather conditions played a dominant role in affecting the interannual variations of agricultural areas (Spangler et al., 2020). For example, the farm crisis of 1980s resulted in a significant cropland drop. Moreover, a series of historical acreage-reduction programs, such as the conservation adjustment act program, cropland acreage-reduction program, and conservation reserve program, resulted in the total cropland reduction (Lubowski et al., 2006). In the recent three decades, the total US cropland has kept relatively constant, but the crop commodities changed significantly. Corn and soybean gradually became the predominant types due to the rising demand for corn as biofuel and the higher market price for soybean, which pushed framers to convert other types to corn and soybean (Bigelow and Borchers, 2017; Aguilar et al., 2015). Overall, the US cropland experienced significant growth between the 1850s and 1920s, driven by population growth, industrialization, mechanization, and market change. It subsequently underwent a process of stabilization after experiencing fluctuations in crop types and area.

4.3 The implications for cropping diversity change

In general, the US cropping diversity experienced a dramatic change throughout the entire period. From 1850 to 1963, it constantly increased (Figure 6 (a)), which was primarily attributed to the area rises from all major crop types at this stage (Figure 3). Spatially, the diversity increases in Southwest, Southeast, and Great Plains promoted the US crop diversity increase (Figure 6(b) and 10). From 1960s to 2021, the cropping diversity had a significant decrease mainly due to the increased planting area for corn and soybean and the decreased cultivated area for winter wheat, spring wheat, sorghum, and barley. Meanwhile, the diversity drop in the Northern Great Plains, Southwest, Southeast, and Midwest might contribute to the US crop diversity decline (Figure 6 (b) and 10). This finding shows a strong agreement with the results of Aguilar et al. (2015), in which the crop species diversity declined from 1980s to 2010s in the Heartland Resource Region.

On the other hand, crop species diversity is an important component of biodiversity in a cropping system and the decreased crop species diversity always accompanies the decreased biodiversity (Altieri, 1999). Some researchers have pointed out that the biodiversity plays an essential role in the functioning of real-world ecosystem. High biodiversity would increase soil fertility, mitigate the impact of pests and diseases, improve resilience to climate change, and promote food production and nutrition security(Altieri, 1999; Duffy, 2009; Frison et al., 2011). For example, Delphine and David's research indicated that crop species diversity could stabilize food production (Renard and Tilman, 2019), and Emily et al. (2019) found that agricultural diversification can increase crop production. Thus, had this significant drop in the US cropping diversity in the past six decades affected yield and ecosystem productivity? Moreover, under more frequent climate extremes anticipated in the future, whether the decreasing cropping diversity will affect the sustainability and resilience of the US agricultural system is an important question to answer.

https://doi.org/10.5194/essd-2023-195
Preprint. Discussion started: 12 September 2023

Open Access Earth System Science Data Discussions

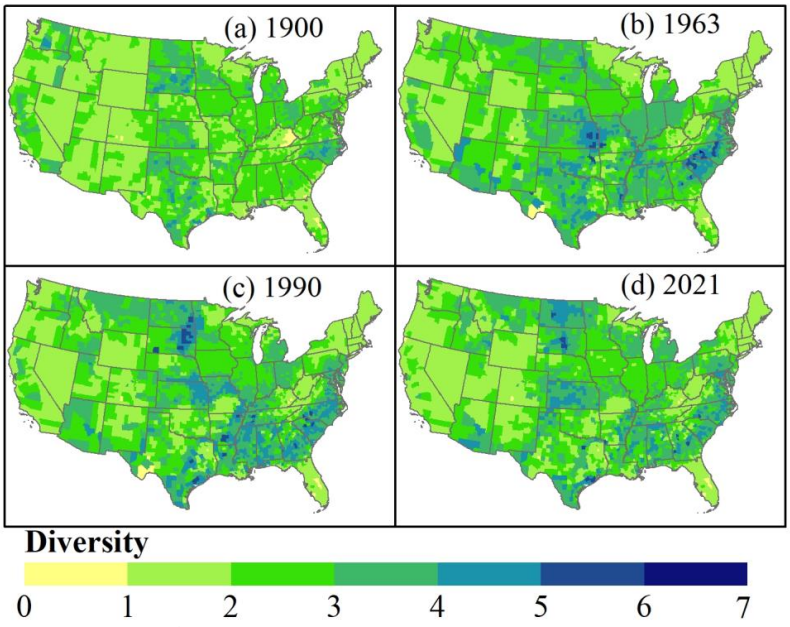

Figure 10. The spatial pattern of crop diversity in 1900, 1963, 1990, and 2021 at the county level. The diversity value is calculated based on the gap-filled and multi-source harmonized inventory data in each county.

4.4 Uncertainty

In this study, we integrated the inventory data and the gridded LUCC products to generate annual cropland density and crop type maps at a resolution of 1 km×1km from 1850 to 2021. Although our data is highly consistent with inventory data, some uncertainties remain:

(1) In the upscaling process of CDL from 30m to 1km, we assigned each pixel to a crop type with the biggest fraction of land area within the pixel. Although the cropland area of each crop was constrained by the inventory data at the county level, this resampling process may ignore some crop type distribution with minor fraction within pixel.

(2) The inventory is crucial for reconstructing historical cropland maps. Here, the rebuilt inventory data in missing years is interpolated, which might ignore some real interannual cropland area fluctuations, causing the final cropland map to misrepresent the annual spatial cropland shift in these years.

(3) In the process of spatializing crop types, we randomly convert the cropland grids from specific types with higher cropland area than inventory data to other crop types in each county. Moreover, the grids identified to have corn-soybean rotation were randomly selected within a county based on corn-soybean rotation ratio, which can help avoid a grid cell being occupied by a fixed crop type over time. Although the extent of the random processes varied among counties depending on the difference between intermediate map data and inventory data, they might affect the temporal trajectory of grid-based crop type changes. Thus, the users should be cautious to use this data product to conduct time sequencing analyses such as crop rotation patterns (e.g., continuous corn, corn-soybean-corn, etc.) at the pixel level.

https://doi.org/10.5194/essd-2023-195
Preprint. Discussion started: 12 September 2023

(4) The diversity in this study mainly reflects ten crop types' diversity change (nine major types and one category of "others"). The "others" in the study is not a single crop type, but a combined category including many other crop types (peanuts, oats, etc.). Thus, the diversity change quantified in this study reflect the diversity of major row crops (accounting for 70% of the national total cropland area in the 2010s) and "others-as-one-category" in the US over time. A more comprehensive diversity analysis involving all crop types needs a more detailed time-series crop type record which is lacking now.

5 Data availability

The developed dataset is available at https://doi.org/10.6084/m9.figshare.22822838.v1(Ye et al., 2023). This dataset includes annual cropland density map and crop type map with Geotiff format at 1km by 1km spatial resolution.

6 Conclusion

In this study, the annual cropland density and crop type map from 1850 to 2021 in the conterminous US was developed by integrating the multi-source cross-scale inventory and gridded datasets. In general, our maps have a high consistency with inventory data both at the national level (R^2>0.99, *RMSE* <0.3 Mha) and county level (R^2>0.98, *RMSE* <4 Kha). Compared with other datasets, the spatial pattern of the developed maps matches well with YLMAP and GBC. Throughout the study period, the total US cropland increased by 118 Mha, mainly driven by corn (30 Mha), soybean (35 Mha), and others (31 Mha). The hot spots have shifted from the East to the Midwest and the Great Plains. Specifically, the Homestead Act of 1862 significantly contributed to the cropland expansion toward the west, and the rising demand for biofuel and the market price resulted in the dramatical increase of corn and soybean planting areas. Meanwhile, the intensified corn and soybean substituted other crops, leading to the decrease of the cropping diversity in the Midwest, which may further influence crop yield and co-benefit of agroecosystem services. Additionally, there were random processes in generating crop type maps. This might bring uncertainty to pixel-based crop type sequence applications, but the area for each crop type was well constrained by gap-filled long-term inventory data. The county-level area control also makes the developed map capable of depicting regional spatial shifts within state. Different from previous datasets, the cropland in our products refers to the planting area of all the crops, excluding idle/fallow farm land, and cropland pasture. Hence, the cropland map provides reliable cultivated information and reveals the surface disturbance conducted by agricultural activities, which can improve the estimation of cropland change's impact on climate change. Overall, the developed datasets provide a historical cropland distribution pattern and fill the data gap in lacking long-term crop extent and type maps. We envision this database could better support the US agricultural management data development with crop-specific information, as well as improve the environmental assessment and socioeconomic analysis related to agriculture activities.

https://doi.org/10.5194/essd-2023-195
Preprint. Discussion started: 12 September 2023

Acknowledgments. This work is supported partially by NSF grant (1903722), NSF CAREER (1945036), and USDA AFRI Competitive grant (1028219).

Author contributions: CL designed the research; SC and PY implemented the research and analyzed the results; SC, PY, and CL wrote and revised the paper.

Competing interests. At least one of the (co-)authors is a member of the editorial board of Earth System Science Data.

References

Aguilar, J., Gramig, G. G., Hendrickson, J. R., Archer, D. W., Forcella, F., and Liebig, M. A.: Crop species diversity changes in the United States: 1978-2012, PLoS One, 10, 1–14, https://doi.org/10.1371/journal.pone.0136580, 2015.

Aizen, M. A., Aguiar, S., Biesmeijer, J. C., Garibaldi, L. A., Inouye, D. W., Jung, C., Martins, D. J., Medel, R., Morales, C. L., Ngo, H., Pauw, A., Paxton, R. J., Saez, A., and Seymour, C. L.: Global agricultural productivity is threatened by increasing pollinator dependence without a parallel increase in crop diversification, Glob. Chang. Biol., 25, 3516–3527, https://doi.org/10.1111/gcb.14736, 2019.

Altieri, M. A.: The ecological role of biodiversity in agroecosystems, Agric. Ecosyst. Environ., 74, 19–31, https://doi.org/10.1016/S0167-8809(99)00028-6, 1999.

Anderson, H. L.: That Settles It: The Debate and Consequences of the Homestead Act of 1862, Hist. Teacher, 45, 117–137, 2011.

Arneth, A., Barbosa, H., Benton, T., Calvin, K., Calvo, E., Connors, S., Cowie, A., Davin, E., Denton, F., and van Diemen, R.: IPCC special report on climate change, desertification, land degradation, sustainable land management, food security, and greenhouse gas fluxes in terrestrial ecosystems, Summ. Policy Makers. Geneva Intergov. Panel Clim. Chang., 2019.

Betts, R. A., Falloon, P. D., Goldewijk, K. K., and Ramankutty, N.: Biogeophysical effects of land use on climate: Model simulations of radiative forcing and large-scale temperature change, Agric. For. Meteorol., 142, 216–233, https://doi.org/https://doi.org/10.1016/j.agrformet.2006.08.021, 2007.

Bigelow, D. and Borchers, A.: Major uses of land in the United States, 2012, 2017.

Boryan, C., Yang, Z., Mueller, R., and Craig, M.: Monitoring US agriculture: the US Department of Agriculture, National Agricultural Statistics Service, Cropland Data Layer Program, Geocarto Int., 26, 341–358, https://doi.org/10.1080/10106049.2011.562309, 2011.

Burchfield, E. K., Nelson, K. S., and Spangler, K.: The impact of agricultural landscape diversification on U.S. crop production, Agric. Ecosyst. Environ., 285, https://doi.org/10.1016/j.agee.2019.106615, 2019.

Cao, B., Yu, L., Li, X., Chen, M., Li, X., Hao, P., and Gong, P.: A 1 km global cropland dataset from 10 000 BCE to 2100 CE, Earth Syst. Sci. Data, 13, 5403–5421, https://doi.org/https://doi.org/10.5194/essd-13-5403-2021, 2021.

https://doi.org/10.5194/essd-2023-195
Preprint. Discussion started: 12 September 2023

527 Driscoll, A. W., Leuthold, S. J., Choi, E., Clark, S. M., Cleveland, D. M., Dixon, M., Hsieh, M., Sitterson, J., and
528 Mueller, N. D.: Divergent impacts of crop diversity on caloric and economic yield stability, Environ. Res. Lett., 17,
529 https://doi.org/10.1088/1748-9326/aca2be, 2022.
530 Duffy, J. E.: Why biodiversity is important to the functioning of real-world ecosystems, Front. Ecol. Environ., 7,
531 437–444, https://doi.org/https://doi.org/10.1890/070195, 2009.
532 Foley, J. A., DeFries, R., Asner, G. P., Barford, C., Bonan, G., Carpenter, S. R., Chapin, F. S., Coe, M. T., Daily,
533 G. C., Gibbs, H. K., Helkowski, J. H., Holloway, T., Howard, E. A., Kucharik, C. J., Monfreda, C., Patz, J. A., Prentice,
534 I. C., Ramankutty, N., and Snyder, P. K.: Global consequences of land use, Science (80-.)., 309, 570–574,
535 https://doi.org/10.1126/science.1111772, 2005.
536 Frison, E. A., Cherfas, J., and Hodgkin, T.: Agricultural biodiversity is essential for a sustainable improvement
537 in food and nutrition security, Sustainability, 3, 238–253, https://doi.org/10.3390/su3010238, 2011.
538 Gaudin, A. C. M., Tolhurst, T. N., Ker, A. P., Janovicek, K., Tortora, C., Martin, R. C., and Deen, W.: Increasing
539 Crop Diversity Mitigates Weather Variations and Improves Yield Stability, PLoS One, 10,
540 https://doi.org/10.1371/journal.pone.0113261, 2015.
541 Goldewijk, K. K., Beusen, A., Doelman, J., and Stehfest, E.: Anthropogenic land use estimates for the Holocene
542 - HYDE 3.2, Earth Syst. Sci. Data, 9, 927–953, https://doi.org/10.5194/essd-9-927-2017, 2017.
543 Hijmans, R. J., Choe, H., and Perlman, J.: Spatiotemporal Patterns of Field Crop Diversity in the United States,
544 1870–2012, Agric. Environ. Lett., 1, 160022, https://doi.org/10.2134/ael2016.05.0022, 2016.
545 Homer, C., Dewitz, J., Jin, S., Xian, G., Costello, C., Danielson, P., Gass, L., Funk, M., Wickham, J., Stehman,
546 S., Auch, R., and Riitters, K.: Conterminous United States land cover change patterns 2001–2016 from the 2016
547 National Land Cover Database, ISPRS J. Photogramm. Remote Sens., 162, 184–199,
548 https://doi.org/https://doi.org/10.1016/j.isprsjprs.2020.02.019, 2020.
549 Johnson, D. M.: A 2010 map estimate of annually tilled cropland within the conterminous United States, Agric.
550 Syst., 114, 95–105, https://doi.org/10.1016/j.agsy.2012.08.004, 2013.
551 Klein Goldewijk, K., Beusen, A., van Drecht, G., and de Vos, M.: The HYDE 3.1 spatially explicit database of
552 human-induced global land-use change over the past 12,000 years, Glob. Ecol. Biogeogr., 20, 73–86,
553 https://doi.org/https://doi.org/10.1111/j.1466-8238.2010.00587.x, 2011.
554 L Jost: Entropy and di v ersity, Opinion, 2, 363–375, 2006.
555 Lambin, E. F. and Meyfroidt, P.: Global land use change, economic globalization, and the looming land scarcity,
556 Proc. Natl. Acad. Sci. U. S. A., 108, 3465–3472, https://doi.org/10.1073/pnas.1100480108, 2011.
557 Lark, T. J.: Interactions between U.S. biofuels policy and the Endangered Species Act, Biol. Conserv., 279,
558 109869, https://doi.org/10.1016/j.biocon.2022.109869, 2023.
559 Li, X., Tian, H., Lu, C., and Pan, S.: Four-century history of land transformation by humans in the United States
560 (1630-2020): annual and 1gkm grid data for the HIStory of LAND changes (HISLAND-US), Earth Syst. Sci. Data,
561 15, 1005–1035, https://doi.org/10.5194/essd-15-1005-2023, 2023.
562 Lubowski, R. N., Vesterby, M., Bucholtz, S., Baez, A., and Roberts, M. J.: Major uses of land in the United States,
563 2002, 2006.

https://doi.org/10.5194/essd-2023-195
Preprint. Discussion started: 12 September 2023

564 Meinig, D. W.: Shaping of America. Vol. 2, Continental America, 1800-1967: A Geographical Perspective on
565 500 Years of History, Yale University Press, 1993.
566 Monfreda, C., Ramankutty, N., and Foley, J. A.: Farming the planet: 2. Geographic distribution of crop areas,
567 yields, physiological types, and net primary production in the year 2000, Global Biogeochem. Cycles, 22, 1–19,
568 https://doi.org/10.1029/2007GB002947, 2008.
569 De Noblet-Ducoudré, N., Boisier, J. P., Pitman, A., Bonan, G. B., Brovkin, V., Cruz, F., Delire, C., Gayler, V.,
570 Van Den Hurk, B. J. J. M., Lawrence, P. J., Van Der Molen, M. K., Müller, C., Reick, C. H., Strengers, B. J., and
571 Voldoire, A.: Determining robust impacts of land-use-induced land cover changes on surface climate over North
572 America and Eurasia: Results from the first set of LUCID experiments, J. Clim., 25, 3261–3281,
573 https://doi.org/10.1175/JCLI-D-11-00338.1, 2012.
574 Ouyang, W., Song, K., Wang, X., and Hao, F.: Non-point source pollution dynamics under long-term agricultural
575 development and relationship with landscape dynamics, Ecol. Indic., 45, 579–589,
576 https://doi.org/10.1016/j.ecolind.2014.05.025, 2014.
577 Ramankutty, N. and Foley, J. A.: Estimating historical changes in land cover North American croplands from
578 1850 to 1992, Glob. Ecol. Biogeogr., 8, 381–396, https://doi.org/10.1046/j.1365-2699.1999.00141.x, 1999.
579 Ramankutty, N., Evan, A. T., Monfreda, C., and Foley, J. A.: Farming the planet: 1. Geographic distribution of
580 global agricultural lands in the year 2000, Global Biogeochem. Cycles, 22,
581 https://doi.org/https://doi.org/10.1029/2007GB002952, 2008.
582 Renard, D. and Tilman, D.: National food production stabilized by crop diversity, Nature, 571, 257+,
583 https://doi.org/10.1038/s41586-019-1316-y, 2019.
584 Spangler, K., Burchfield, E. K., and Schumacher, B.: Past and Current Dynamics of U.S. Agricultural Land Use
585 and Policy, Front. Sustain. Food Syst., 4, 1–21, https://doi.org/10.3389/fsufs.2020.00098, 2020.
586 Tang, F. H. M., Nguyen, T. H., Conchedda, G., Casse, L., and Tubiello, F. N.: CROPGRIDS : A global geo-
587 referenced dataset of 173 crops circa 2020, 22491997, 1–22, 2023.
588 Tilman, D., Balzer, C., Hill, J., and Befort, B. L.: Global food demand and the sustainable intensification of
589 agriculture, Proc. Natl. Acad. Sci. U. S. A., 108, 20260–20264, https://doi.org/10.1073/pnas.1116437108, 2011.
590 Turner, B. L.: The earth as transformed by human action, Prof. Geogr., 40, 340–341, 1988.
591 Vanwalleghem, T., Gomez, J. A., Amate, J. I., de Molina, M. G., Vanderlinden, K., Guzman, G., Laguna, A., and
592 Giraldez, J. V: Impact of historical land use and soil management change on soil erosion and agricultural sustainability
593 during the Anthropocene, ANTHROPOCENE, 17, 13–29, https://doi.org/10.1016/j.ancene.2017.01.002, 2017.
594 Waisanen, P. J. and Bliss, N. B.: Changes in population and agricultural land in conterminous United States
595 counties, 1790 to 1997, Global Biogeochem. Cycles, 16, https://doi.org/10.1029/2001GB001843, 2002.
596 Xian, G. Z., Smith, K., Wellington, D., Horton, J., Zhou, Q., Li, C., Auch, R., Brown, J. F., Zhu, Z., and Reker,
597 R. R.: Implementation of the CCDC algorithm to produce the LCMAP Collection 1.0 annual land surface change
598 product, Earth Syst. Sci. Data, 14, 143–162, https://doi.org/10.5194/essd-14-143-2022, 2022.
599 Yang, J., Tao, B., Shi, H., Ouyang, Y., Pan, S., Ren, W., and Lu, C.: Integration of remote sensing, county-level
600 census, and machine learning for century-long regional cropland distribution data reconstruction, Int. J. Appl. Earth

https://doi.org/10.5194/essd-2023-195
Preprint. Discussion started: 12 September 2023

601 Obs. Geoinf., 91, 102151, https://doi.org/10.1016/j.jag.2020.102151, 2020.
602 Ye, S., Cao, P., and Lu, C.: Annual time-series 1-km maps of crop area and types in the conterminous US
603 (CropAT-US) during 1850-2021, https://doi.org/10.6084/m9.figshare.22822838.v1, 2023.
604 Yu, Z. and Lu, C.: Historical cropland expansion and abandonment in the continental U.S. during 1850 to 2016,
605 Glob. Ecol. Biogeogr., 27, 322–333, https://doi.org/10.1111/geb.12697, 2018.
606 Yu, Z., Lu, C., Cao, P., and Tian, H.: Long-term terrestrial carbon dynamics in the Midwestern United States
607 during 1850-2015: Roles of land use and cover change and agricultural management, Glob. Chang. Biol., 24, 2673–
608 2690, https://doi.org/10.1111/gcb.14074, 2018.
609 Zhang, W., Ricketts, T. H., Kremen, C., Carney, K., and Swinton, S. M.: Ecosystem services and dis-services to
610 agriculture, Ecol. Econ., 64, 253–260, https://doi.org/https://doi.org/10.1016/j.ecolecon.2007.02.024, 2007.
611 Zumkehr, A. and Campbell, J. E.: Historical U.S. cropland areas and the potential for bioenergy production on
612 abandoned croplands, Environ. Sci. Technol., 47, 3840–3847, https://doi.org/10.1021/es3033132, 2013.
613